PROCEEDINGS, Thirty-Ninth Workshop on Geothermal Reservoir Engineering
Stanford University, Stanford, California, February 24-26, 2014
SGP-TR-202

Thermal Performance of Directional Wells for EGS Heat Extraction

Elena A. Kalinina, Teklu Hadgu, Katherine A. Klise, and Thomas S. Lowry

Sandia National Laboratories, MS 1369, P.O. Box 5800, Albuquerque, NM 87185, USA

e-mail: eakalin@sandia.gov

Keywords: geothermal reservoir simulation; enhanced geothermal systems; heat extraction; horizontal and directional wells; reservoir permeability; fracture orientation; fracture properties; injection interval.

ABSTRACT

The purpose of this research is to investigate the potential of Enhanced Geothermal Systems (EGS) heat extraction using directional wells. Analyses of EGS systems have typically assumed vertical well configurations that are set up in either a 2-point, 3-point, or 5-point injection scheme. Our previous research (Kalinina et al., 2012a and 2012b) demonstrates that the performance of vertical wells is greatly affected by the well separation, thickness of the injection interval, vertical anisotropy in reservoir permeability, and fracture properties and orientation. The near-vertical orientation of fractures often found in EGS environments means that vertical wells cannot optimally exploit the geothermal resources. In addition, vertical well performance can be impacted by density differences that cause the colder injected water to sink to the bottom of the injection interval.

The potential of directional well drilling to overcome these problems has led to an investigation of their thermal and economic performance across a variety of EGS environments. This paper presents the thermal performance results of that investigation. The economic evaluation is considered in "Economic Valuation of Directional Wells for EGS Heat Extraction", Lowry et al. (2014).

1. INTRODUCTION

Directional drilling technology achieved commercial viability during the late 1980's (EIA, 1993). This technology has significantly advanced over the past decades. This was mainly due to a large demand for these wells in oil exploration industry. The directional wells provide access to formations that are not accessible with vertical drilling and are especially useful in offshore locations. The use of directional wells in oil exploration has been constantly growing due to significant increase in the reservoir productivity that can be achieved with these wells. While a directional well can be two or more times as expensive as a vertical well directed to the same target horizon, the economic benefits related to the increased reservoir productivity may outweigh the additional costs.

The latest technological advances made in directional drilling allow for achieving large horizontal displacements and shorter distances to bend from vertical to horizontal directions. The costs of drilling directional wells have been going down as a result of improvements in technology.

Even though most directional wells are drilled in carbonate rocks, the existing technology can be adopted for EGS conditions. The major question is whether the directional wells offer a significant improvement in heat extraction compared to conventional vertical wells and whether the improvements are worth the added costs. This study focuses on answering the first question while the evaluation of the associated economic benefits is considered in Lowry et al. (2014).

2. MODELING SETUP

The design specifications and cost estimation of drilling and completing directional wells in conditions typical for EGS were developed for Sandia National Laboratories by Baker Hughes. The design package and cost breakdown were developed for vertical and directional wells. The directional wells included the following profiles:

i. "J" type well with tangent inclination of 45° (inclined well)
ii. Horizontal well with sail angle of 90°

The costs were estimated using current drilling, labor and material rates. Cost breakout followed accepted oil and gas industry standards. The design specifications and cost estimates mainly rely upon industry best practices and, as such, are preliminary. However, they provide a good starting point for considering applications of directional wells in EGS exploration.

The well design proposed by Baker Hughes is based on the following assumptions:

- The EGS reservoir is located within the depth interval of 1,600 m to 3,200 m.
- The reservoir rock is either granite, granodiorite, or basalt with a rock density of 2,850 kg/m^3.

- The overlying formation is either claystone, siltstone, or sandstone with the rock density of 2,650 kg/m^3.
- Reservoir temperature is 200^{0}C.
- The directional control is maintained while drilling through hard and possibly fractured igneous rocks.

The design assumed a pair of two vertical or directional wells with the profiles described above and with a production liner of up to 1,400 m long.

To provide consistency between the heat extraction analysis and economic evaluation, the modeling setup adopted the Baker Hughes design specifications and corresponding parameters. The injection scheme consisted of one injection well and one production well with a base separation distance of 800 m. To incorporate this injection scheme, the modeling domain encompassing an EGS reservoir was represented with a rectangle 1,600 m wide (*X* axis), 400 m deep (*Y* axis) and 1,600 tall (*Z* axis). The top of the modeling domain was assumed to be at a 1600 m depth below ground surface. The same model grid cell size of 15 m was used in each direction. The modeling domain consists of 338,256 cells.

The EGS reservoir properties depend on the natural fracture network and on the changes to this network induced by the reservoir stimulation. This results in highly heterogeneous conditions with significant degree of uncertainty in spatial variations of the reservoir permeability. In the absence of actual data, a number of different reservoir representations must be considered.

The fracture continuum model (FCM) approach described in detail in Kalinina et al. (2012a) was used to generate different EGS reservoir representations. This approach allows for representing reservoir permeability using the fracture network data and is applicable to both natural and stimulated conditions.

The permeability values in *X*, *Y*, and *Z* directions are calculated for each model grid block based on the fracture aperture, spacing, strike, and dip probability distributions for each fracture set. The continuous fractures are created by introducing spatial correlation in the direction of fracture strike and dip. Depending on the correlation length, the fracture can extend over a few model blocks or over the entire modeling domain.

The probability distributions of the following fracture set parameters are required for generating permeability fields:

- Fracture strike
- Fracture dip
- Fracture aperture
- Fracture spacing

In this study we assumed that the natural fracture network consists of one fracture set. The fracture set includes multiple fractures with similar strike and dip values. Different strikes and dips were considered to account for the uncertainty in the reservoir properties as described below.

Two orientations of the fracture set were considered: approximately aligned (80^0) with the *X* axis and approximately aligned (10^0) with *Y* axis (the well-pair plane simulated in the model is along the *X* axis). A few different values of the average dip were considered: 75^0, or 18^0, or 5^0. Strike and dip were represented by normal distributions with the mean values provided above and standard deviations of 3^0.

An exponential distribution was assigned to the fracture spacing with a mean value of 1.0 m, a minimum value of 0.1 m, and maximum value of 15 m. The same distribution was used for all the different reservoir representations.

A normal distribution was assigned to fracture aperture with a mean aperture of 0.1 mm and a standard deviation of 0.01 mm.

To model the stimulate conditions, it is assumed that stimulation will only widen the existing fractures and that the fracture spacing will remain the same. Two stimulation scenarios were considered, a ‘moderate stimulation’ where the mean fracture aperture was set equal to 0.22 mm, and a ‘significant stimulation’, where the mean fracture aperture was set equal to 0.47 mm.

The fracture parameter distributions defined above are based on our previous literature review of granite properties (Kalinina et al., 2012a and 2013) supplemented with the additional data collected since that time. The previous data included the granite rock sites that have been studied worldwide for many different purposes, such as potential disposal of radioactive wastes; mining (quarry development); contaminant transport; and oil and gas exploration. The additional data (Cladouhos, 2011; Murphy et al., 1980; Kosack et al., 2011a&b; McClure, 2009; Saito and Hayashi, 2002; Tenma et al., 2008, Huenges et al., 2011, and Wyborn, 2011) targeted specifically the geothermal reservoirs.

The additional data are consistent with the following conclusions made based on the previous data:

- Mean fracture spacing is 0.3 m to 3.0 m.
- The spacing probability distribution is either power law or exponential.
- The fracture aperture follows a normal distribution.
- The observed fracture aperture ranges from 0.5 mm to 1.5 mm with larger apertures corresponding to stimulated conditions.

The average permeability values of the natural fracture network obtained with the fracture parameters specified above were $2.2x10^{-13}$ m^2 in i_1 direction, $2.4x10^{-13}$ m^2 in i_2 direction, and $2.3x10^{-14}$ m^2 in i_3 direction. The direction (i_1, i_2, or i_3) was a function of the fracture dip and orientation. For example, when fracture strike was 10^0 and fracture dip was 18^0, i_1= *X*, i_2=*Y*, and i_3=*Z*.

The average permeability values under the moderately stimulated conditions were $2.2x10^{-12}$ m^2 in i_1 direction, $2.4x10^{-12}$ m^2 in i_2 direction, and $2.3x10^{-13}$ m^2 in i_3 direction. The average permeability values under the significantly stimulated conditions were $2.2x10^{-11}$ m^2 in i_1 direction, $2.4x10^{-11}$ m^2 in i_2 direction, and $2.3x10^{-11}$ m^2 in i_3 direction.

As a comparison, the estimated permeability values in the different parts of the Soultz EGS reservoir were $1.1x10^{-13}$ m^2; $2.4x10^{-13}$ m^2; and $2.8x10^{-13}$ m^2 (Kosack et al., 2011a). These values are consistent with the average values defined for the natural fracture network.

Different combinations of fracture strike, dip, spacing, and aperture resulted in different permeability fields or reservoir representations. These permeability fields are representative of the expected reservoir conditions because they are based on the probability distributions of the parameter common for granite rocks.

Figure 1 shows an example of the simulated values of strike, dip, spacing, and fracture aperture for the natural fracture network with the average strike of 10^0 and average dip of 18^0. These values are calculated for each of 338,256 blocks representing the modeling domain.

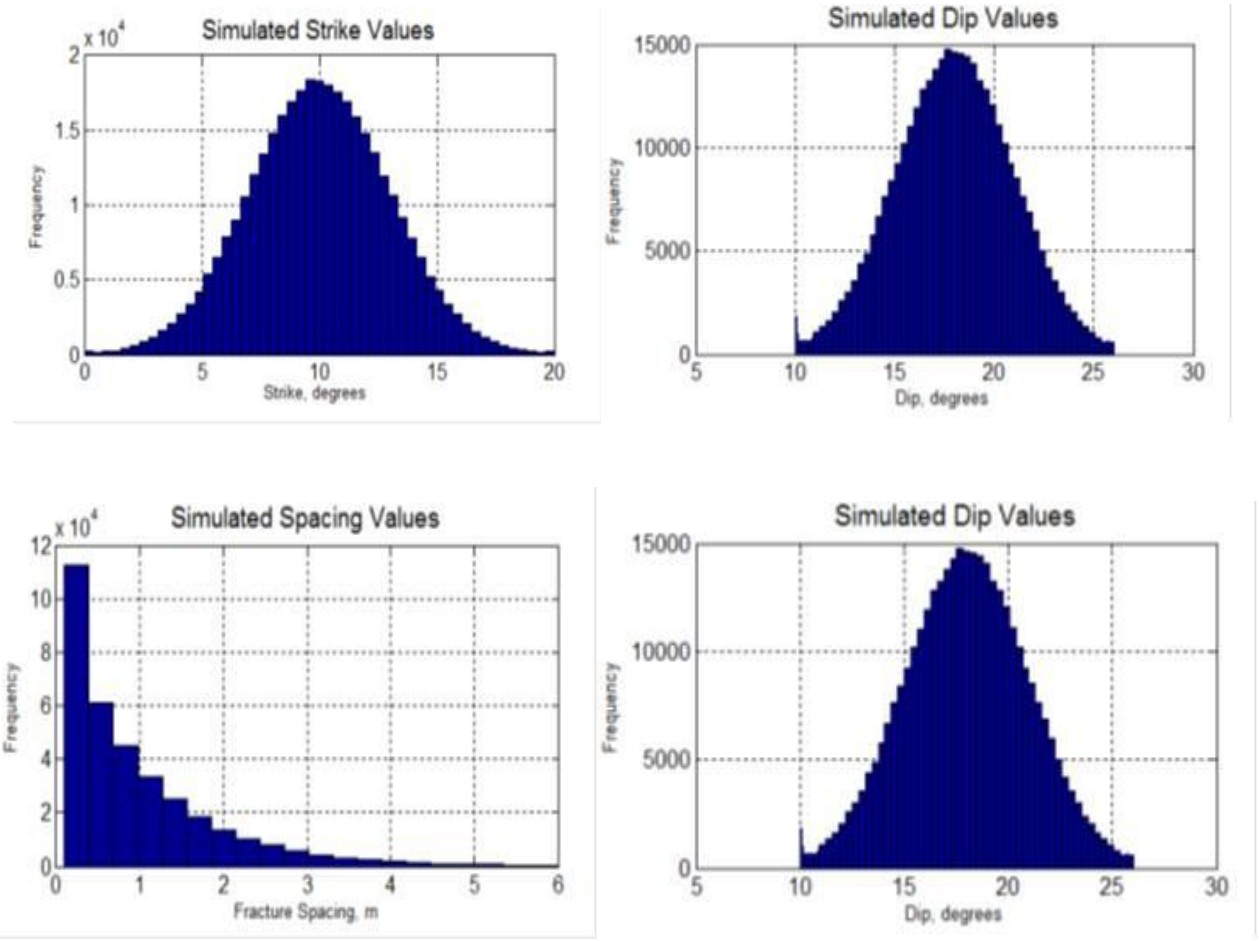

Figure 1: Simulated values of fracture parameters for the natural fracture network with 10° strike and 18° dip.

Figure 2 shows the permeability field for the permeability in *X* direction (K_x) for the same example. Similar fields are obtained for K_y and K_z values.

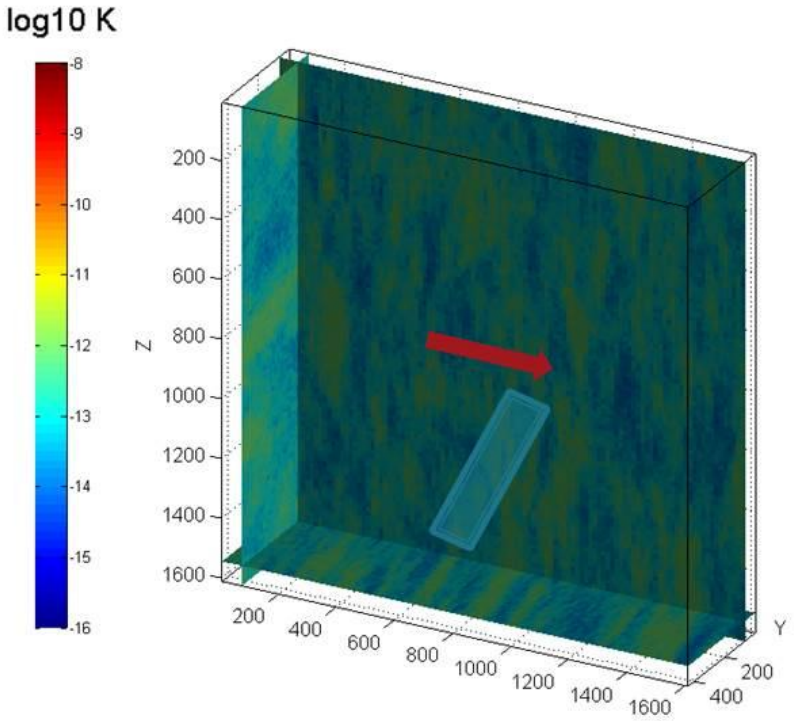

NOTE: Blue rectangle shows the predominant fracture plane and the red arrow shows the direction of injection in the vertical well setup. *Z*=0 at the reservoir top (1,600 m below the ground).

Figure 2: Permeability field (K_x) for the natural fracture network with 10° strike and 18° dip.

The K_x, K_y, and K_z values were calculated for each grid cell and for each reservoir representation and were written in the format required for the heat transport simulations with the Finite Element Heat and Mass Transfer code FEHM (Zyvoloski, 1997).

The heat transport problem was considered for one injector and one producer scheme. The temperature of the injected water was set to 80^0C. The base injection rate was 120 kg/s. The initial hydrostatic pressures in the modeling domain were calculated for each permeability field assuming constant reservoir temperature (200^0C). All the boundaries during the injection were set as impermeable boundaries with no credit for geothermal (temperature) gradient at the reservoir bottom.

The setups for the vertical and horizontal wells are shown in Figure 3. In both cases, the setups differ by the injection interval length. The following injection interval lengths were considered:

1. 1400 m
2. 1000 m
3. 750 m
4. 500 m
5. 250 m

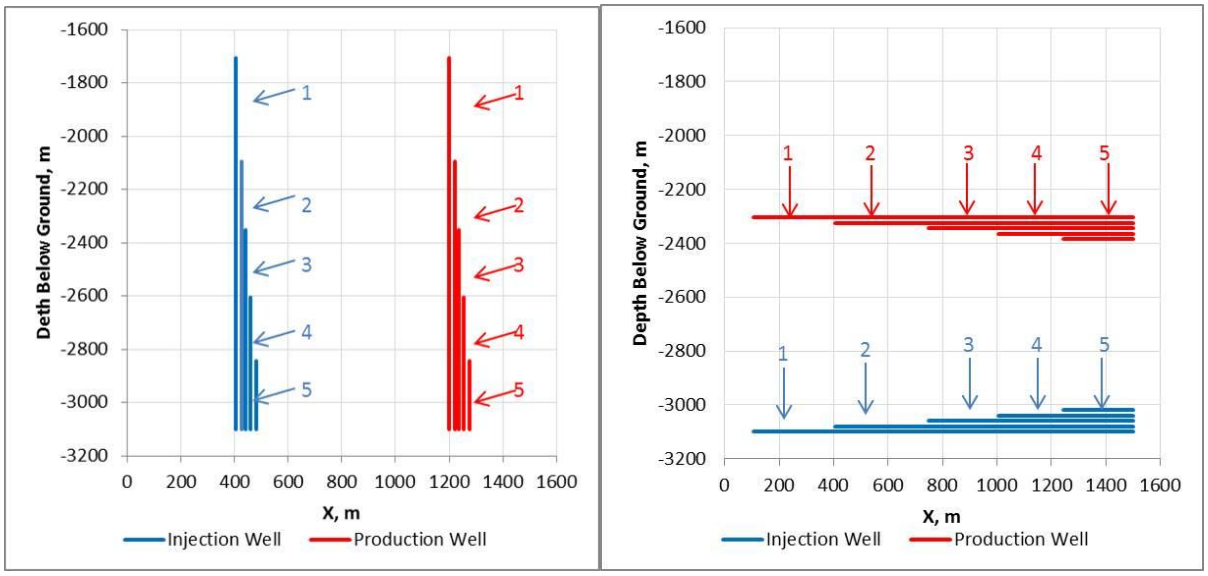

NOTE: each setup is designated a number (for example, the setup 1 is for the injection interval 1,400 m). The wells are located along the same vertical lines and are shown with a small separation for illustration purpose only.

Figure 3: Injection and production intervals considered in the vertical and horizontal well setups, respectively.

The setup for the inclined wells is shown in Figure 4. The vertical and horizontal wells setups used to compare the heat extraction performance in these cases are shown in this figure as well.

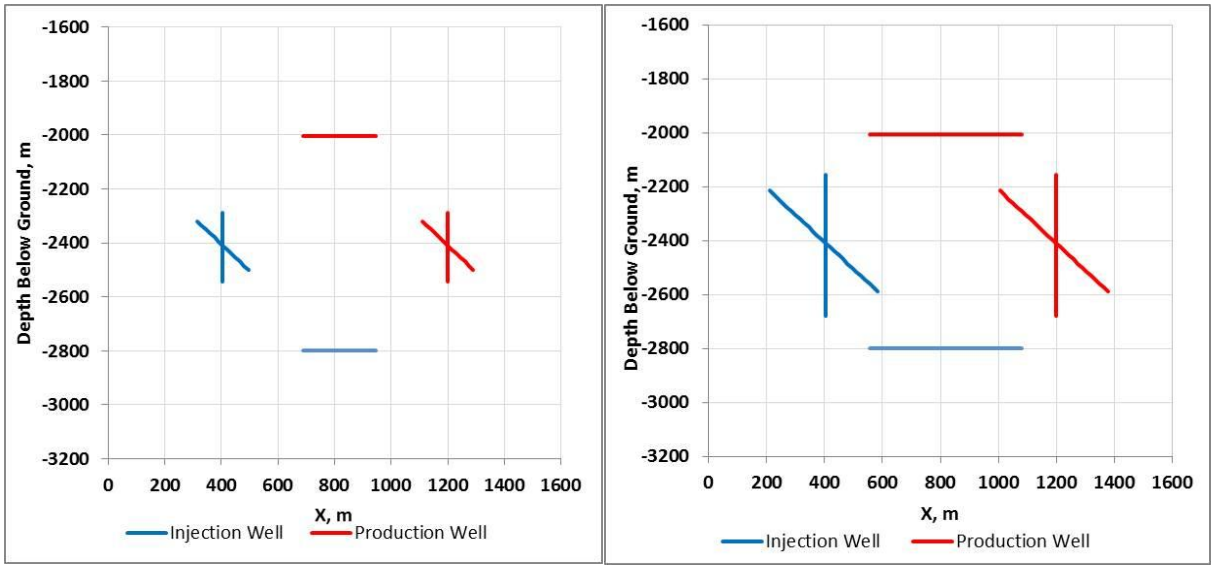

NOTE: Figure on left is for the injection interval length of 250 m and figure on right is for the injection interval length of 525 m

Figure 4: Injection and production intervals considered in the inclined well setups and vertical and horizontal wells used for comparison.

The injection and production wells were modeled by specifying the injection/production internal boundary condition in the model nodes that fall within the injection/production intervals shown in Figures 3 and 4.

The average temperature in the production well is a function of the fluid enthalpy and mass in each node representing the well. To calculate the average temperature we applied heat and mass balance at each node. The mass averaged enthalpy at each time step (h_{ave}) can be calculated as:

$$h_{ave} = \frac{\sum_1^n h_i q_i}{\sum_1^n q_i} \quad (1)$$

where n, h_i, q_i are the number of nodes representing the production well, the node enthalpy, and the mass flow exiting the node, respectively.

The mass averaged enthalpy (h_{ave}) is then converted to the average production temperature using steam table relations (Harr et al., 1984).

The performance of each well setup scheme was evaluated for the different reservoir representations in terms of average temperature in the production well during the 30 year injection period. The discussion of the simulation results is provided below.

3. SIMULATION RESULTS

The simulation results include the output from over 100 runs. These runs were designed to evaluate the heat extraction performance as a function of the following factors:

- Injection interval length
- Fracture orientation (strike and dip)
- Well separation distance
- Stimulation conditions

3.1 Injection Interval Length

One of the common features of granite rocks is highly variable fracture density with depth (Dezayes, 2000; Genter and Traineau, 1992; Sausse, 2001). As a result, the intervals with high fracture density suitable for injection may have limited thickness. In our simulations we assumed that the injection interval length ranges from 250 m to 1,400 m. The maximum production rates achieved so far in the EGS exploration indicate that the injection interval length must be much smaller than 1,400 m.

Figure 5 shows the average temperature histories in the production well in the vertical and horizontal well setups as a function of the injection interval length. The results shown in this figure is for the natural fractures with strike of 80^0 and dip of 18^0. Similar results were obtained for the other reservoir representations.

The production temperature in the vertical well case is strongly affected by the injection interval length (Figure 5). The production temperature drop is large and the performance of heat extraction is poor when the injection interval length is below 750 m.

The injection interval length in the horizontal well case has virtually no effects on the production temperature (Figure 5).

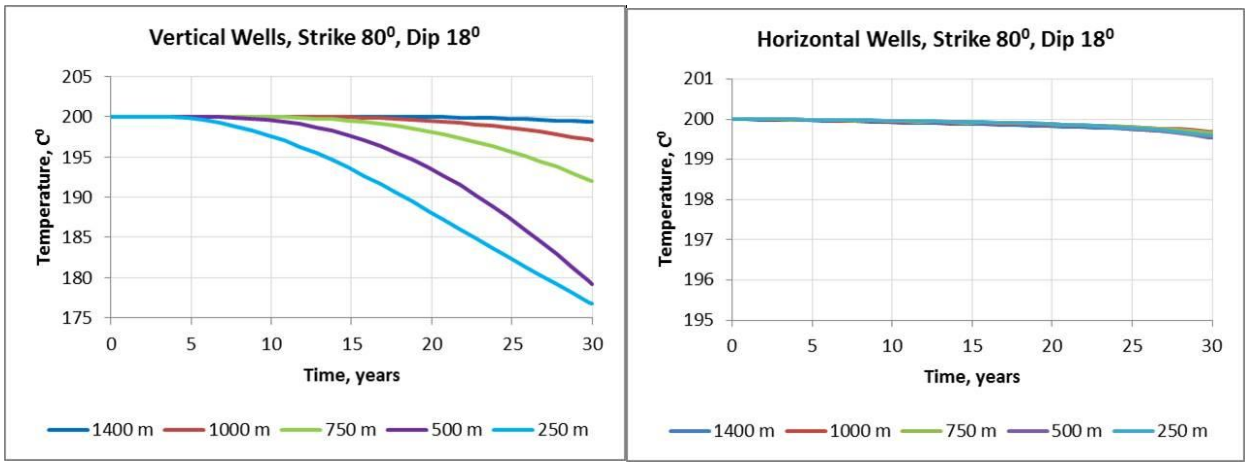

Figure 5: Average temperature in the production well as a function of injection interval length for the vertical and horizontal well setup, respectively.

3.2 Fracture Orientation

The properties of a fracture network are among the most uncertain parameters. Even when the actual borehole data are available, the degree of uncertainty in spatial variability is often very high. Consequently, it is important to understand how this uncertainty can affect the heat extraction. The following four combinations of fracture strikes and dips were considered to address this uncertainty:

- Strike 80^0, dip 75^0
- Strike 80^0, dip 18^0
- Strike 80^0, dip 5^0
- Strike 10^0, dip 18^0

Figures 6 through 8 show the average temperature histories in the production well in the vertical, inclined, and horizontal well setups as a function of the fracture properties.

The production temperature in the vertical and inclined well cases is strongly affected by the dip and orientation of the fracture network (Figures 6 and 7).

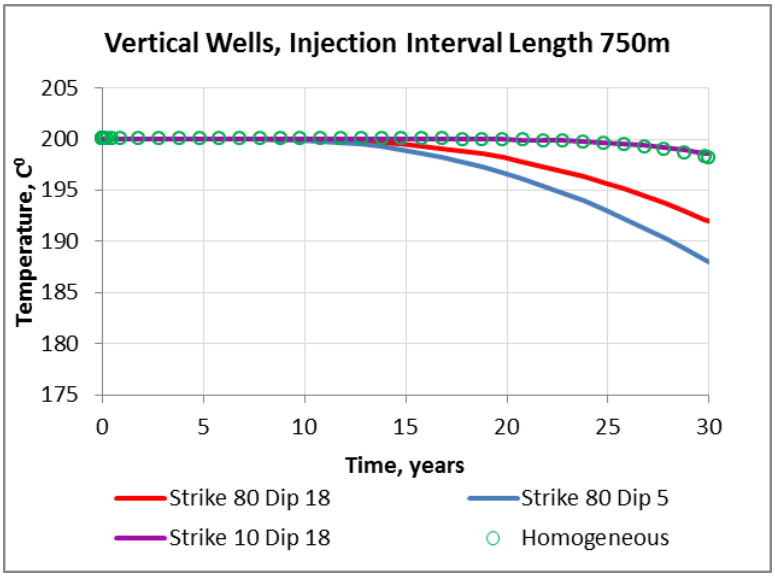

Figure 6: Average temperature in the production well in the vertical well setup as a function of fracture orientation.

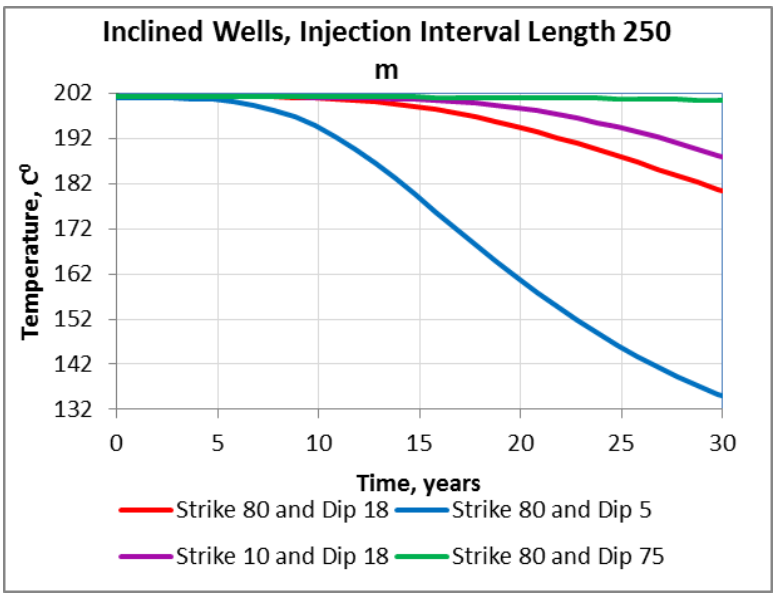

Figure 7: Average temperature in the production well in the inclined well setup as a function of fracture orientation.

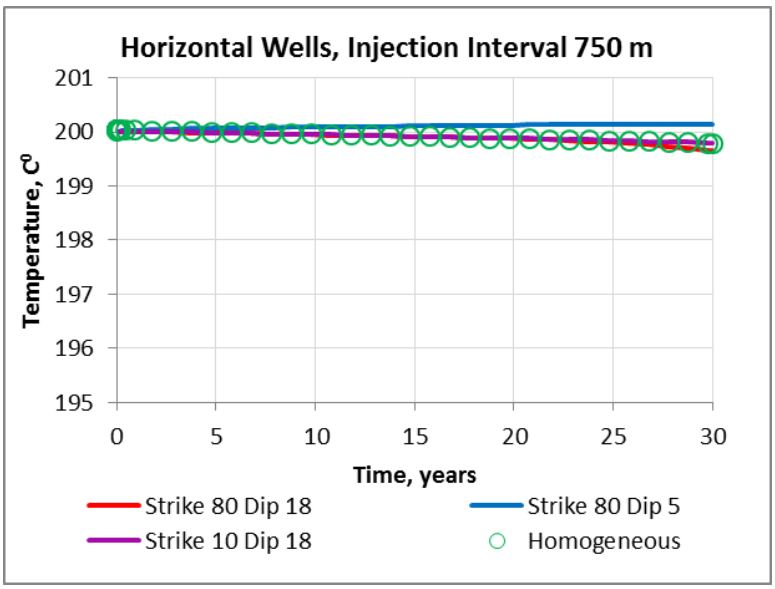

Figure 8: Average temperature in the production well in the horizontal well setup as a function of fracture orientation.

Figures 6 and 8 also show the average production temperatures calculated using an equivalent homogeneous anisotropic reservoir representation and show that assuming homogeneous reservoir conditions may lead to over estimating the heat extraction performance in the vertical well case.

3.3 Well Separation Distance

The well separation distance is one of a few factors that, to some extent, are controllable. Generally, the larger the well separation, the more heat can be extracted. However, the maximum distance might be limited by the reservoir extent, the achievable stimulation radius, and the potential pumping requirements. As an example, the separation distances are 650 m at Soultz (Sausse, 2008), 200 m at Fenton Hill (Murphy et al., 1980), 400 m at Urach (,Huenges et al., 2011) and 500 and 568 m at Habanero (Wyborn, 2011). The practical range for EGS exploration seems to be from 300 m to 1,000 m.

Figures 9 and 10 show the average temperature histories in the production well in the vertical and horizontal well setups as a function of the well separation distance. The separation distances of 390 m and 600 m were considered in addition to the base case separation distance of 800 m.

The production temperature in the vertical well cases is strongly affected by the separation distance (Figure 9). The production temperatures for the 800 m separation and 600m separation are only slightly different in the horizontal well case (Figure 10). The separation distance of 390 m results in a temperature drop of 9^0C after 30 years of injection for the horizontal configuration, and 52^o C for the vertical configuration.

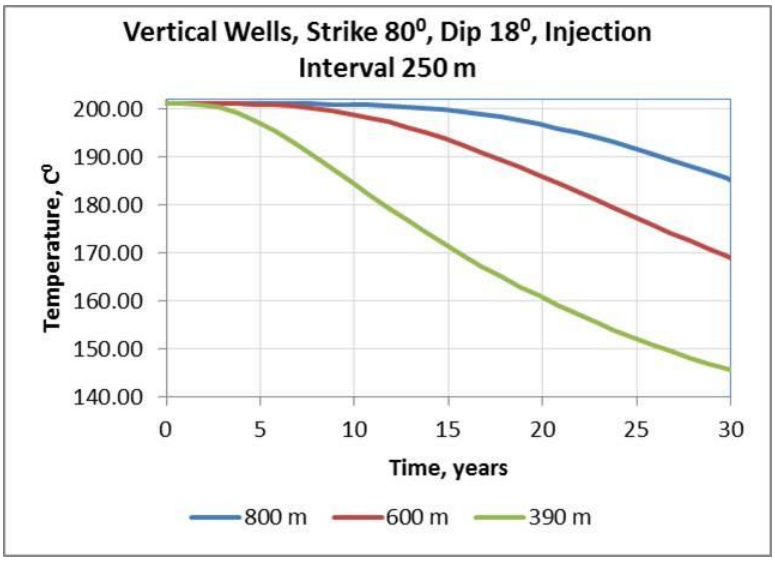

Figure 9: Average temperature in the production well in the vertical well setup as a function of separation distance.

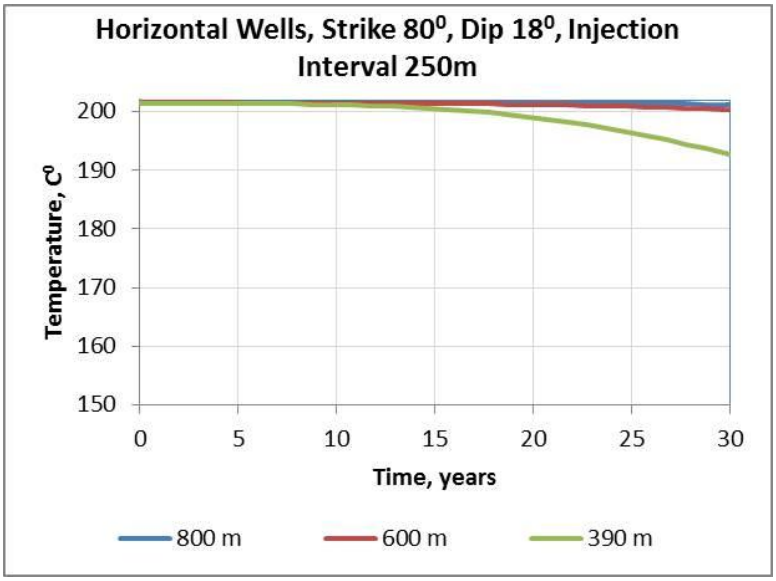

Figure 10: Average temperature in the production well in the horizontal well setup as a function of separation distance.

3.4 Stimulation Conditions

The major goal of the stimulation is to increase reservoir permeability either by widening (re-opening) the fractures in the existing natural fracture network or by creating new fractures. In this analysis, we assumed that the reservoir permeability ($2x10^{-13}$ m^2) was increased by a factor of 10 in the moderate stimulation case and by factor of 100 in the high stimulation case. These increased permeability values are assumed to be due to widening of the fracture apertures. As it was previously discussed, the average fracture apertures are assumed to be 220 μm in the moderate stimulation and 470 μm in the significant stimulation.

Figures 11 and 12 show the average temperature histories in the production well in the vertical and horizontal well setups as a function of the average reservoir permeability.

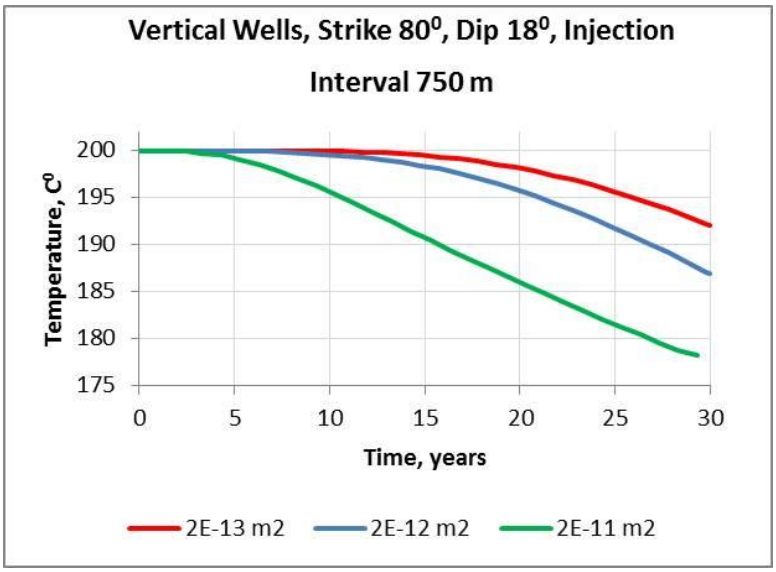

Figure 21: Average temperature in the production well in the vertical well setup as a function of reservoir permeability.

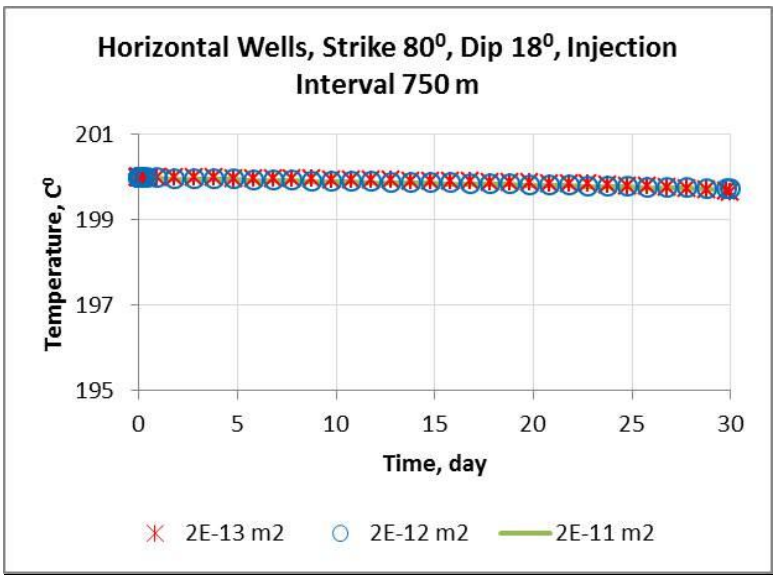

Figure 32: Average temperature in the production well in the horizontal well setup as a function of reservoir permeability.

In this case, the reservoir stimulation does not result in a better heat extraction in the vertical well case (Figure 11).

The heat extraction in the horizontal well case is not affected by the stimulation conditions (Figure 12). However, high pressure differences between the injection and production wells were calculated when the fracture dip was 5^0 because the vertical permeability was 10 times lower than horizontal ones. This specific case would require a moderate stimulation to increase vertical permeability.

In both cases, stimulating the reservoir will impact pumping requirements and hence the economic viability of each scenario. This will be discussed in more detail in the accompanying paper.

The problem with the reservoir stimulation in the vertical well case is illustrated in Figure 13. The time and temperature scales in this figure are intentionally not shown. The performance of a moderately stimulated reservoir is better than the performance of an unstimulated reservoir after time t_1. The performance of a highly stimulated reservoir is better than the performance of an unstimulated reservoir after time t_2. The performance of a highly stimulated reservoir is better than the performance of moderately stimulated reservoir after time t_3. The unstimulated reservoir performs better than stimulated ones until time t_1 or t_2. The moderately stimulated reservoir performs better than highly stimulated one until the time t_3. There are no benefits in stimulation if t_1 and t_2 are close to the end of the injection period. The significant benefit can be only achieved if t_1 and t_2 are close to the beginning of injection.

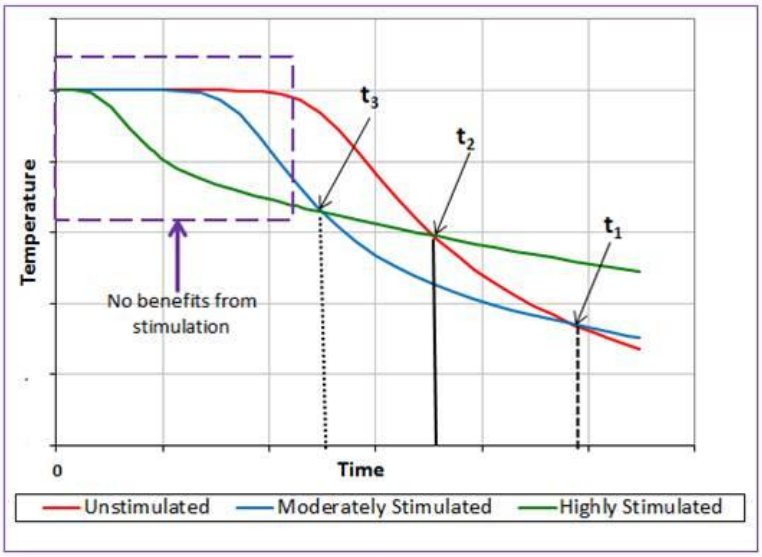

Figure 43: Illustration of stimulation impacts on the reservoir heat extraction performance for vertical wells.

As an example, the simulation results shown in Figure 11 fall within the purple rectangle labeled 'No benefit from stimulation'.

The times t_1 and t_2 are affected by the injection rate, separation distance, injection interval length, and fracture properties. As a result, it is not easy to predict whether the stimulation will be successful

3.5 Vertical versus Horizontal Well Setups

A better performance of horizontal wells compared to vertical and inclined ones can be explained using the temperature field at the end of the injection (Figure 14) as an example.

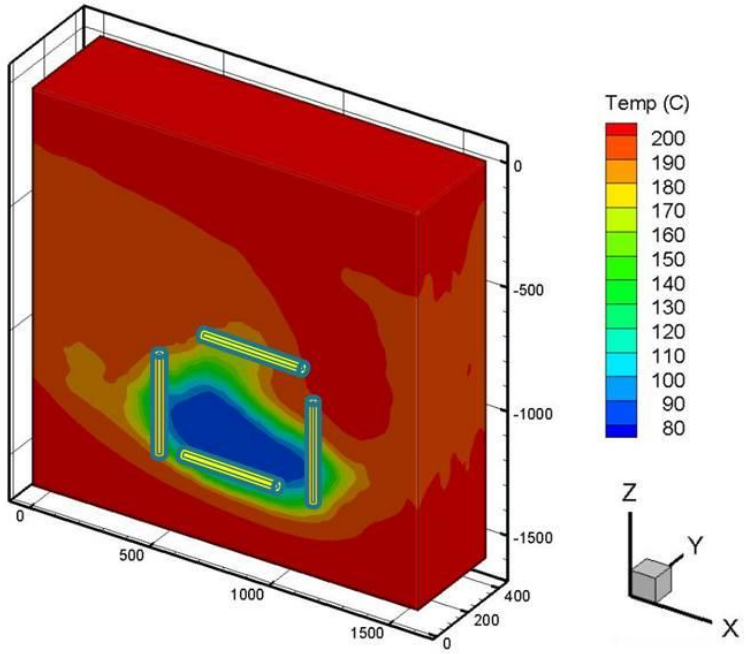

NOTE: Z=0 at the reservoir top (1,600 m below the ground).

Figure 54: Distribution of temperature at the end of simulation, horizontal well, well separation distance 800 m.

As Figure 14 illustrates, the cold water spreads much faster in the horizontal directions than in the vertical direction. As a result, the production well temperature in the vertical well is impacted to a much larger extent than the production well temperature in the horizontal well.

4. CONCLUSIONS

The ability of the vertical wells to extract heat from an EGS reservoir is significantly affected by the length of the injection interval, well separation distance, fracture properties, and stimulation. To maintain acceptable average temperature in the production well during the injection period, the injection interval length and well separation distance should be large and the spatial distribution of the fracture properties within the reservoir should be well understood. Furthermore, reservoir stimulation does not necessarily guarantee better heat extraction.

The heat extraction performance with the inclined wells is affected by the same factors as the vertical wells. The inclined wells perform better than vertical in some cases and worse than vertical in other ones.

The heat extraction with the horizontal wells is practically not affected by the length of the injection interval and fracture properties within the parameter ranges considered in this analysis. The parameter ranges were selected to represent the common properties of the granite rocks and injection setups.

Under most of the conditions considered in this analysis, the stimulation was not required in the horizontal well case. Some stimulation might be required if there are layers with the low fracture density within the injection interval.

The main factor that affects the performance of the horizontal wells was the well separation distance. This effect is only noticeable for the separation distance of 400 m or less. Even in this case, the decrease in the average production well temperature by the end of injection is relatively small (9^0C).

This study demonstrated that the horizontal well setup allows for reducing the risks associated with the following factors:

- The uncertainty in fracture parameters and their spatial distribution.

- Unsuccessful stimulation.
- Insufficient length of the injection interval.

The exploration and production risk reduction comes at the price of higher costs of the horizontal wells. The economic benefits associated with the horizontal wells are evaluated in the subsequent study presented in Lowry et al. (2014).

ACKNOWLEDGEMENTS

Sandia National Laboratories is a multi-program laboratory managed and operated by Sandia Corporation, a wholly owned subsidiary of Lockheed Martin Corporation, for the U.S. Department of Energy's National Nuclear Security Administration under contract DE-AC04-94AL85000.

REFERENCES

Cladouhos, T.T., Clyne, M., Nichols, M., Petty, S., Osborn, W.L. and Nofziger, L.: Newberry Volcano EGS Demonstration Stimulation Modeling, Geothermal Resources Council *Transactions*, 35, (2011), 317-322.

McClure, M.W.: Fracture Stimulation in Enhanced Geothermal Systems, Masters of Science thesis, Dept. of Energy Resources Engineering, Stanford University, CA (2009).

Energy Information Administration (EIA): Drilling Sideways -- A Review of Horizontal Well Technology and Its Domestic Application, DOE/EIA-TR-0565, (1993).

Harr, L., Gallagher, J., and. Kell, G.S.: NBS/NRC Steam Tables, Thermodynamics, and Transport Properties and Computer Programs for Vapor and Liquid States of Water, *Hemisphere Press*, (1984).

Murphy, H.D., Tester, J.W., and Potter, R.M.: Comparison of Two Hot Dry Rock geothermal reservoirs, Fenton Hill, Los Alamos, Sixth Annual Workshop on Geothermal Reservoir Engineering Stanford University, Stanford, CA, (1980).

Kalnina, E.A.; Klise, K.A., McKenna, S., Hadgu, T., Lowry, T. S.: Applications of the Fractured Continuum Model (FCM) to EGS Heat Extraction Problems, *Proceedings*, 38th Workshop on Geothermal Reservoir Engineering, Stanford University, Stanford, California, (2013), SGP-TR-198, 845-854.

Kalinina, E, McKenna, S.A., Hadgu, T., Lowry, T.S.: Analysis of the Effects of Heterogeneity on Heat Extraction in an EGS Represented with the Continuum Fracture Model", *Proceedings, 37-th Workshop on Geothermal Reservoir Engineering*, Stanford University, Stanford, California, (2012a), SGP-TR-194, 436-445.

Kalinina, E, McKenna, S.A., Klise, K., Hadgu, T., Lowry, T.S.: Incorporating Complex Three-Dimensional Fracture Network into Geothermal Reservoir Simulations, Geothermal Resources Council *Transactions*, **36**, (2012b), 493-498.

Kosack, C., Rath, V., Mottaghy, D., and Wolf, A.: Parameter Estimation of the Geothermal Reservoir at Soultz-sous-Forêts, *Geophysica*, Beratungsgesellschaft mbH, (2011a).

Kosack, C., Vogt, C., Marquart, G., Clauser, C., and Rath, V: Stochastic Permeability Estimation for the Soultz-Sous-Forets EGS Reservoir, *Proceedings*, Thirty-Sixth Workshop on Geothermal Reservoir Engineering Stanford University, Stanford, California, (2011b), SGP-TR-191.

Genter, A. and Traineau, H.: Hydrothermally Altered and Fractured Granite as an HDR Reservoir in the EPS-1 Borehole, Alsace, France, *Proceedings*, 17-th Workshop on Geothermal Reservoir Engineering, Stanford University, Stanford, California, (1992), SGP-TR-141, 33-38.

Huenges, E., Ledru, P., and Wiley, J. & Sons: Geothermal Energy Systems: Exploration, Development, and Utilization, (2011).

Lowry, T.S., E. Kalinina, T. Hadgu, K. Klise, L.A. Malczynski: Economic Valuation of Directional Wells for EGS Heat Extraction, *Proceedings*, 39th Workshop on Geothermal Reservoir Engineering, Stanford University, Stanford, CA, (2014), SGP-TR-202.

Saito, H. and Hayashi, K.: Hydraulic Properties Evaluation from Stoneley Wave Attenuation by using Permeable Fracture Zone Model, Geothermal Resources Council *Transactions*, Vol. 2 6, (2002).

Sausse, J.: Hydromechanical Properties and Alteration of Natural Fracture Surfaces in the Soultz Granite (Bas-Rhin, France), *Tectonophysics*, Elsevier, (2001).

Sausse, J., Dezayes, C., Genter, A., and Bisset, A.: Characterization of Fracture Connectivity and Fluid Flow Pathways derived from Geological Interpretation and 3D Modelling of the Deep Seated EGS Reservoir of Soultz (France), *Proceedings*, Thirty-Third Workshop on Geothermal Reservoir Engineering Stanford University, Stanford, California, (2008), SGP-TR-185.

Tenma, N., Yamaguchi, T., and Zyvoloski, G.: The Hijiori Hot Dry Rock Test Site, Japan: Evaluation and Optimization of Heat Extraction from a Two-layered Reservoir, *Geothermics*, **37**, (2008), 19–52.

Wyborn, D.: Hydraulic Stimulation of the Habanero Enhanced Geothermal System (EGS), South Australia, *5th BC Unconventional Gas Technical Forum*, (2011).

Zyvoloski, G.A., Robinson, B.A., Dash, Z.V., and Trease, L.L.: Summary of the Models and Methods for the FEHM Application - A Finite-Element Heat- and Mass-Transfer Code, LA-13307-MS, Los Alamos, New Mexico: Los Alamos National Laboratory, (1997).